

Studies on the Electroactive Heterocycles $C_6S_8^{0/2-}$ and $C_6S_6O_2^{0/2-}$ and Related Metal Complexes

Jun-Hong Chou, Thomas B. Rauchfuss,* and Lisa F. Szczepura†

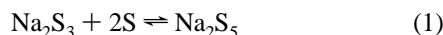
Contribution from the School of Chemical Sciences and the Frederick Seitz Materials Research Laboratory, University of Illinois at Urbana–Champaign, Urbana, Illinois 61801

Received September 10, 1997

Abstract: The properties of the carbon sulfide C_6S_8 (**1**) as well as its dioxo analogue $C_6S_6O_2$ (**2**) have been studied in the fully oxidized and fully reduced forms, i.e., 1^0 , 1^{2-} , 2^0 , 2^{2-} . A crystallographic study shows that compound **2** is a tricyclic species with a twisted 1,2-dithiin (unsaturated C_4S_2 ring) core. Reduction of **1** with 2 equiv of $LiBHET_3$ gave $C_6S_8^{2-}$ (1^{2-}), which was isolated as its PPh_4^+ salt. A crystallographic study of this salt shows that reduction has resulted in cleavage of the S–S bond and that, in the solid state, the dihedral angle between the two rings is 180° . Both 1^{2-} and 2^{2-} undergo two sequential and reversible $1e^-$ oxidations near 0 V (vs Ag/AgCl), thus establishing that 1^0 and 2^0 are good oxidants relative to other disulfides. Treatment of $(PPh_4)_2[C_6S_8]$ with $[Ni(H_2O)_6]Cl_2$ afforded the dark red $(PPh_4)_2[Ni(C_6S_8)_2]$ (**3**). The analogous Pt complex (**4**) was also prepared. Crystallographic analysis of **3** shows that the nickel center is square planar, comprising two seven-membered NiS_2C_4 rings. The paramagnetism observed for solutions of **3** are attributed to the formation of a tetrahedral isomer.

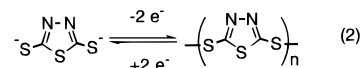
Introduction

The redox behavior of the S–S bond is important in many areas of chemistry.¹ For example, the scission of the S–S bond in lipoic acid derivatives is an essential step in the Krebs Citric Acid Cycle.² The cysteine-cystine equilibrium³ plays a determining role in the tertiary structures of many proteins. Synthetic polymers also have been prepared with redox active S–S linkages in their backbones.^{4,5} Energy storage technologies have been based on the reduction of S–S bonds, e.g., sulfur–sodium batteries.⁶ The charging and discharging cycle in such devices involves the shortening or elongation of polysulfido chains (eq 1).



In recent years, research on the use of sulfur-based batteries has been invigorated through the development of both new cathodes and new anodes.⁷ Of relevance to the present work,

organic disulfides have become of interest as replacement for inorganic sulfur in the cathodes.⁸ The basic redox cycle of the organic disulfides is similar to that involving alkali metal polysulfides, i.e., the reductive cleavage of S–S bonds.⁹ Although the cycling rates of batteries based on organic disulfides is less than that for their inorganic counterparts,¹⁰ the organic disulfides offer a number of advantages including low operating temperatures. In contrast, alkali metal inorganic polysulfides have high melting points which necessitates that the battery operates at temperatures in the 300–400 °C range.¹¹ The organic disulfides are available with a wide range of substituents, thus allowing one to fine-tune the melting point, redox potential, and equivalent weight. Particular attention has focused on the use of polymeric organic disulfides—the so-called solid redox polymerization electrodes (SRPEs). Illustrative is the redox cycle for dimercaptodithiazolate (eq 2).



Since the battery's cell potential is directly related to its energy density, there is interest in the synthesis of new disulfides which are highly oxidizing.

* To whom correspondence should be addressed.

† Current address: Department of Chemistry, Illinois State University, Normal, IL 61790.

(1) Review of lipoic acid and derivatives: Teuber, L. *Sulfur Reports* **1990**, 9, 257. A highly readable overview of cyclic disulfides: Isenberg, N.; Grdinic, M. *J. Chem. Educ.* **1972**, 49, 392.

(2) Reed, J. J.; Hackert, M. L. *J. Biol. Chem.* **1990**, 265, 8971.

(3) Stankovich, M. T.; Bard, A. J. *J. Electroanal. Chem.* **1977**, 75, 487.

(4) Compton, D. L.; Brandt, P. F.; Rauchfuss, T. B.; Rosenbaum, D. F.; Zukoski, C. F. *Chem. Mater.* **1995**, 7, 2342. Compton, D. L.; Rauchfuss, T. B. *Organometallics* **1994**, 13, 4367. Galloway, C. P.; Rauchfuss, T. B. *Angew. Chem., Int. Ed. Engl.* **1993**, 32, 1319. Brandt, P. F.; Rauchfuss, T. B. *J. Am. Chem. Soc.* **1992**, 114, 1926.

(5) For example: Ding, Y.; Hay, A. S. *Macromolecules* **1996**, 29, 6386.

(6) Vincent, C. A.; Bonino, F.; Lazzari, M.; Scrosati, B. *Modern Batteries*; Pu: London, 1987. *Lithium Batteries, New Materials, Developments, Perspectives*; Pistoia, G., Ed.; Elsevier: New York, 1994.

(7) Wilson, A. M.; Zank, G. A.; Eguchi, K.; Xing, W.; Yates, B.; Dahn, J. R. *Chem. Mater.* **1997**, 9, 1601. Armstrong, A. R.; Bruce, P. G. *Nature* **1996**, 381, 499 and references therein.

(8) Liu, M.; Visco, S. J.; De Jonghe, L. C. *J. Electrochem. Soc.* **1991**, 138, 1896. Liu, M.; Visco, S. J.; De Jonghe, L. C. *J. Electrochem. Soc.* **1991**, 138, 1891. Visco, S. J. M., C. C.; De Jonghe, L. C.; Armand, M. B. *J. Electrochem. Soc.* **1989**, 136, 661.

(9) NEXAFS studies establishing that the charging and discharging cycles of the Li-organic disulfide battery involves the formation and breaking of S–S linkages: Yang, X. Q.; Xue, K. H.; Lee, H. S.; Guo, Y. H.; McBreen, J.; Skotheim, T. A.; Okamoto, Y.; Lu, F. *J. Electrochem. Soc.* **1993**, 140, 943.

(10) Blends of the organo sulfur compounds and polyaniline may allow for the commercial development of these batteries, see: Oyama, T. T.; Sato, T. *Sotomura Nature* **1995**, 373, 598. Ye, S.; Bélanger, D. *J. Phys. Chem.* **1996**, 100, 15848.

(11) Kanatzidis, M. G.; Sutorik, A. C. *Prog. Inorg. Chem.* **1995**, 43, 151

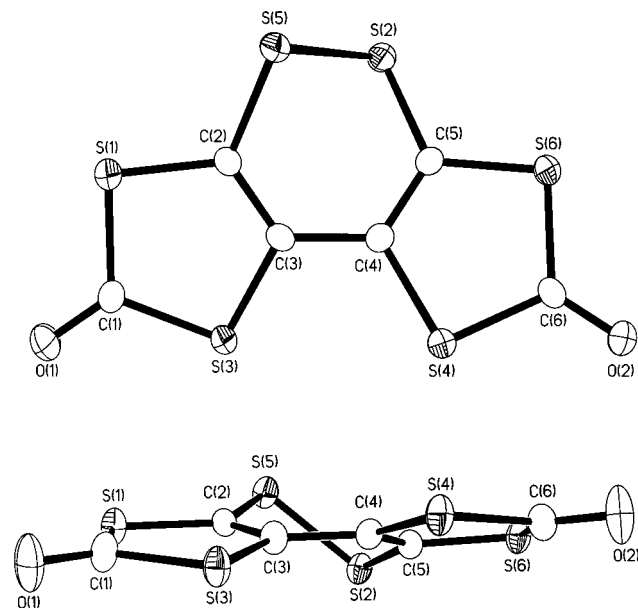
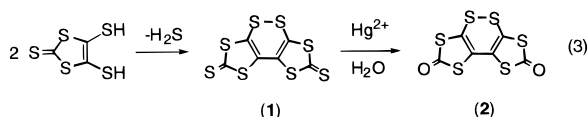


Figure 1. Structure of $C_6S_8O_2$ (2^0) with thermal ellipsoids drawn at the 50% probability level.

The present results are derived from our research on new compositions composed only of sulfur and carbon. Our efforts,^{12–14} and those of others,¹⁵ have resulted in the preparation of several new binary carbon sulfide anions and molecules. An important member of this series is the tricyclic species C_6S_8 , which is the focus of this paper. This species is prepared by the thermal decomposition of $C_3S_5H_2$. The corresponding $C_6S_6O_2$ is easily prepared from C_6S_8 (eq 3). The present studies



on the redox chemistry of C_6S_8 and $C_6S_6O_2$ show the following: (i) that they are exceptionally oxidizing persulfido compounds, (ii) that their electrochemistry is reversible on the time scale of cyclic voltammetry, and (iii) that the reduction products, $C_6S_8^{2-}$ and $C_6S_6O_2^{2-}$, which are 1,4-dimercaptobutadiene derivatives, form stable coordination complexes.

Results

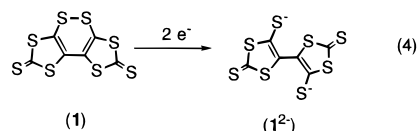
Structural Studies on C_6S_8 and $C_6S_6O_2$. We were initially interested in confirming the structure of at least one of these tricyclic species. We were unable to grow crystals of C_6S_8 (1^0) because of its poor solubility. The related bis(dithiocarbonate) $C_6S_6O_2$ (2^0), following trends noted earlier,¹⁴ is significantly more soluble and crystallized well from organic solvents. Single-crystal X-ray analysis showed that **1** has a tricyclic core and a single S–S bond (Figure 1). The S–S bond length is 2.054(2) Å (Table 1). The linkage C2–C3–C4–C5 exhibits single-double bond alternation as follows: 1.341(6), 1.458(6), 1.353(6) Å, respectively. Perhaps of greatest interest is the C2–S5–S2–C5 dihedral angle of 25.3, the nonplanarity of which

Table 1. Selected Distances (Å) and Angles (Deg) in $C_6S_6O_2$ (2^0) with Standard Deviations in Parentheses

S1–C2	1.745(4)	S1–C1	1.786(5)	S2–C5	1.759(5)
S2–S5	2.054(2)	S3–C3	1.758(4)	S3–C1	1.780(5)
S4–C4	1.755(5)	S4–C6	1.777(5)	S5–C2	1.773(4)
S6–C5	1.743(5)	S6–C6	1.778(5)	O1–C1	1.198(6)
O2–C6	1.202(6)	C2–C3	1.341(6)	C3–C4	1.458(6)
C4–C5	1.353(6)				
C2–S1–C1	96.0(2)	C5–S2–S5	97.9(2)		
C3–S3–C1	96.4(2)	C4–S4–C6	96.3(2)		
C2–S5–S2	97.9(2)	C5–S6–C6	95.8(2)		
O1–C1–S3	123.7(4)	O1–C1–S1	123.9(4)		
S3–C1–S1	112.4(3)	C3–C2–S1	118.3(3)		
C3–C2–S5	122.5(3)	S1–C2–S5	118.9(3)		
C2–C3–C4	124.5(4)	C2–C3–S3	116.8(3)		
C4–C3–S3	118.7(3)	C5–C4–C3	123.0(4)		
C5–C4–S4	116.5(3)	C3–C4–S4	120.5(3)		
C4–C5–S6	118.4(4)	C4–C5–S2	123.2(4)		
S6–C5–S2	118.3(3)	O2–C6–S4	123.4(4)		
O2–C6–S6	123.6(4)	S4–C6–S6	113.0(3)		

gives the molecule idealized C_2 symmetry. Schroth and co-workers have conducted the only other crystallographic characterization of tricyclic 1,2-dithiins (i.e., 1,2-dithiabenzene), where the fused rings are thiophenes. In Schroth's species the dihedral angles for the C–S–S–C linkages are within a 2° of 52° ,¹⁶ i.e., they are much less planar than **2**. In acyclic disulfides, the C–S–S–C dihedral angles are typically 90° .

Synthesis and Properties of $C_6S_8^{2-}$. Suspensions of C_6S_8 in THF dissolve upon the addition of 2 equiv of $LiBHET_3$ ¹⁷ to give violet solutions which contain the dianion 1^{2-} . Addition of methanolic PPh_4Cl to these solutions afforded an almost quantitative yield of violet-black microcrystals of $(PPh_4)_2[C_6S_8]$ (eq 4). This salt can be recrystallized from DMF–Et₂O. The



same reduction can also be achieved using sodium-ammonia solutions. Chemical reduction of **2** with $LiBHET_3$ produces brown colored solutions containing $C_6S_6O_2^{2-}$; this anion was also isolated as its PPh_4^+ salt. The compound, $(PPh_4)_2[C_6S_6O_2]$, or $(PPh_4)_2[2]$, is also soluble in DMF and DMSO.

The 2:1 salts were characterized by several spectroscopic techniques. The ^{13}C NMR spectrum of $(PPh_4)_2[1]$ features three resonances for the anion at δ 207.3, 159.2, and 123.7, assigned to the thiocarbonyl and two olefinic carbon centers, respectively. The corresponding ^{13}C NMR spectrum of $(PPh_4)_2[2]$ displays three resonances at δ 196.6, 148.4, and 111.6 in DMSO-*d*₆, all three of which are slightly shifted with respect to $C_6S_8^{2-}$. The IR spectrum of $(PPh_4)_2[1]$ exhibits strong bands at 1439 and 1024 cm^{-1} , assigned to $cm^{-1} \nu_{C=C}$ and $\nu_{C=S}$, respectively. These salts exhibit rich optical spectra.

This structure of $(PPh_4)_2C_6S_8$ was confirmed by single-crystal X-ray diffraction (Figure 2). The anion is centrosymmetric, consisting of a butadiene-like C_4 chain terminated in cyclic trithiocarbonates and bearing thiolato groups at C2 and C2A. The greatest difference between 2^{2-} and its neutral parent, aside

(12) Chou, J.-H.; Rauchfuss, T. B. *J. Am. Chem. Soc.* **1997**, *119*, 4537.

(13) Galloway, C. P.; Doxsee, D. D.; Fenske, D.; Rauchfuss, T. B.; Wilson, S. R.; Yang, X. *Inorg. Chem.* **1994**, *33*, 4537.

(14) Doxsee, D. D.; Galloway, C. P.; Rauchfuss, T. B.; Wilson, S. R.; Yang, X. *Inorg. Chem.* **1993**, *32*, 5467.

(15) Gompper, R.; Knieler, R.; Polborn, K. *Z. Naturforsch.* **1993**, *48b*, 1621. Bock, H.; Näther, C.; Rauschenbach, A.; Havlas, Z.; Bats, J. W.; Fanghanel, E.; Palmer, T. *Phosphorus, Sulfur, Silicon* **1994**, *91*, 53.

(16) Kempe, R.; Sieler, J.; Hintzsche, E.; Schroth, W. *Z. Kristallogr.* **1993**, *208*, 145. Schroth, W.; Hintzsche, E.; Felicetti, M.; Spitzner, R.; Sieler, J.; Kempe, R. *Angew. Chem., Int. Ed. Engl.* **1994**, *33*, 739. Schroth, W.; Hintzsche, E.; Viola, H.; Winkler, R.; Klose, H.; Boese, R.; Kempe, R.; Sieler, J. *Chem. Ber.* **1994**, *127*, 401.

(17) Gladys, J. A.; Wong, V. K.; Jick, B. G. *Tetrahedron* **1979**, *35*, 2329.

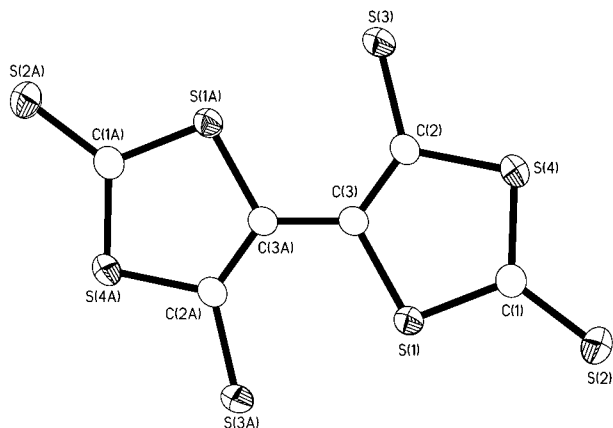


Figure 2. Structure of the anion 2^{2-} in $(\text{PPh}_4)_2[\text{C}_6\text{S}_8]$ with thermal ellipsoids drawn at the 50% probability level.

Table 2. Selected Distances (Å) and Angles (deg) for the Anion 1^{2-} in $(\text{Ph}_4\text{P})_2[\text{C}_6\text{S}_8]$ with Standard Deviations in Parentheses

S1—C1	1.726(2)	S1—C3	1.779(2)	S2—C1	1.674(2)
S3—C2	1.718(2)	S4—C1	1.704(2)	S4—C2	1.751(2)
C2—C3	1.384(2)	C3—C3	1.446(3)		
C1—S1—C3	98.10(9)	C1—S4—C2	99.57(9)		
S2—C1—S4	124.9(1)	S2—C1—S1	122.2(1)		
S4—C1—S1	112.9(1)	C3—C2—S3	130.3(2)		
C3—C2—S4	114.7(1)	S3—C2—S4	115.0(1)		
C2—C3—C3	126.2(2)	C2—C3—S1	114.6(1)		
C3—C3—S1	119.1(2)				

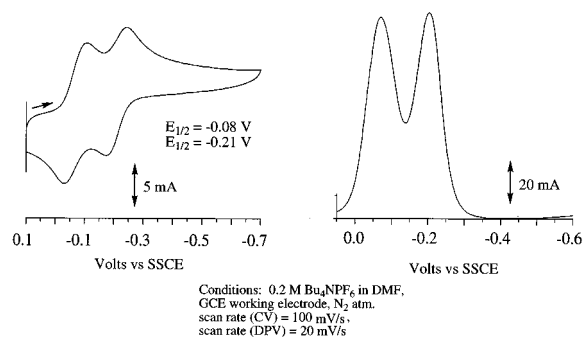


Figure 3. Cyclic voltammogram of $(\text{PPh}_4)_2\text{C}_6\text{S}_6\text{O}_2$ (2^{2-}) and differential pulse voltammogram of $\text{C}_6\text{S}_8\text{O}_2$ (2), both for DMF solutions.

from the cleaved S—S bond, is the fact that reduction has resulted in rotation by 180° about the central C—C bond. The C—C bonds are relatively localized, with alternating single and double bonds between these four carbon atoms (Table 2).

Electrochemical Studies. The electrochemical properties of 1^{2-} , 2^0 , and 2^{2-} were examined by cyclic voltammetry on DMF solutions. Using a glassy carbon electrode, solutions of 2^0 exhibit reversible couples at -0.07 and -0.21 V vs SSCE (saturated sodium calomel electrode). This reversibility is evident from the relative values of the peak anodic and cathodic currents (Figure 3). There is a linear dependence of the peak currents (i_{pa}) on $(\nu)^{1/2}$ over the range of 50 – 400 mV/s, indicating that the processes are reversible and diffusion controlled. Complementary electrochemical studies were conducted on the dianions 1^{2-} and 2^{2-} , each of which displayed two oxidative couples at 0.09 and -0.06 V and at -0.07 and -0.21 V vs SSCE, respectively. These couples also show reversible behavior. Preparative scale oxidation of a MeOH slurry of 1^{2-} with bromine gave a precipitate of C_6S_8 , as confirmed by the IR spectrum of the isolated solid.

Although we defer to a future more detailed report, some general aspects of the half oxidized species, e.g., 1^- and 2^- ,

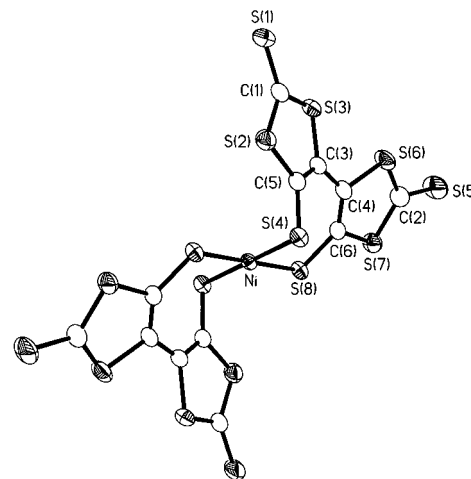
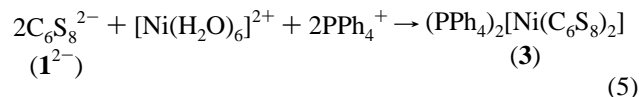


Figure 4. Structure of the anion in $(\text{PPh}_4)_2[\text{Ni}(\text{C}_6\text{S}_8)_2]$ (3) with thermal ellipsoids drawn at the 50% probability level.

are evident from the CV data. Using the calibration curve provided by Richardson and Taube for differential pulse voltammograms of two-electron couples,¹⁸ $\Delta E_{1/2}$ for the two redox couples in 1 was determined to be 142 mV. The stability of the intermediate species, 1^- , can be expressed by the comproportionation constant, K_{com} , which was calculated using the equation $\log K_{\text{com}} = \Delta E_{1/2}/0.0591$ to be 214 . These data indicates that solutions of 1^- (or $(1)_2^{2-}$) should be relatively free of the 1^0 and 1^{2-} . A future report will deal with the characterization of the monoanion.¹⁹

Studies on $[\text{M}(\text{C}_6\text{S}_8)_2]^{2-}$. As a further means of manipulating the redox behavior of the thiolato centers in 2 , we examined the properties of two simple metal complexes. The complex $(\text{PPh}_4)_2[\text{Ni}(\text{C}_6\text{S}_8)_2]$ (3) was prepared by combining DMF solutions of $(\text{PPh}_4)_2[\text{C}_6\text{S}_8]$ and methanolic solution of $[\text{Ni}(\text{H}_2\text{O})_6]\text{Cl}_2$ (eq 5).²⁰ $(\text{PPh}_4)_2[\text{Ni}(\text{C}_6\text{S}_8)_2]$ is a dark reddish brown



compound that dissolves in a variety of polar and weakly polar organic solvents. The compound is relatively air stable. In its IR spectrum, the band at 1434 cm^{-1} is assigned as $\nu_{\text{C}=\text{C}}$. We also isolated the analogous complex $(\text{PPh}_4)_2[\text{Pt}(\text{C}_6\text{S}_8)_2]$ (4) via the reaction of 1^{2-} with K_2PtCl_4 .

The crystallographic analysis of 3 confirms the presence of Ni^{2+} in a square planar coordination sphere defined by four thiolato sulfur atoms (Figure 4, Table 3). The seven-membered $\text{C}_4\text{S}_2\text{Ni}$ ring is puckered, and the two C_3S_2 rings are twisted out of coplanarity with a dihedral angle of 37.8° . The easy formation of the nickel complex indicates that the rotation about the C3—C4 bond has a low barrier.

Whereas square planar nickel(II) complexes are diamagnetic, solutions of 3 are clearly paramagnetic. Attempts to record the ^{13}C NMR spectrum of the complex were unsuccessful, although strong signals were seen for the phenyl carbon atoms of the PPh_4^+ cations. Solution magnetic measurements on CH_2Cl_2 solutions gave a moment of $1.05 \mu_{\text{B}}$ under ambient conditions. Since CH_2Cl_2 is poorly coordinating, the paramagnetism is attributed to the formation of a complex of tetrahedral geometry, as might be expected in light of the tetrahedral geometry observed for $\text{Ni}(\text{SPH})_4^{2-}$.²¹ In contrast, the corresponding platinum complex remains diamagnetic in solution indicating

(18) Richardson, D. E.; Taube, H. *Inorg. Chem.* **1981**, *20*, 1278.

Table 3. Selected Distances (Å) and Angles (deg) the Anion in $(\text{Ph}_4\text{P})_2[\text{Ni}(\text{C}_6\text{S}_8)_2]$ (**3**) with Standard Deviations in Parentheses

Ni-S8	2.1987(6)	Ni-S4	2.2457(5)	S1-C1	1.647(3)
S2-C1	1.728(3)	S2-C5	1.756(2)	S3-C1	1.732(3)
S3-C3	1.760(2)	S4-C5	1.731(2)	S5-C2	1.650(3)
S6-C2	1.717(3)	S6-C4	1.765(2)	S7-C2	1.727(3)
S7-C6	1.766(2)	S8-C6	1.736(2)	C3-C5	1.359(3)
C3-C4	1.450(3)	C4-C6	1.368(3)		
S8-Ni-S8	180.0	S8-Ni-S4	91.74(2)		
S8-Ni-S4	88.26(2)	S4-Ni-S4	180.0		
C1-S2-C5	98.6(1)	C1-S3-C3	98.4(1)		
C5-S5-Ni	94.44(8)	C2-S6-C4	98.6(1)		
C2-S7-C6	99.3(1)	C6-S8-Ni	116.29(8)		
S1-C1-S2	125.6(2)	S1-C1-S3	122.4(2)		
S2-C1-S3	112.0(2)	S5-C2-S6	122.7(2)		
S5-C2-S7	125.1(2)	S6-C2-S7	112.1(1)		
C5-C3-C4	127.5(2)	C5-C3-S3	115.4(2)		
C6-C4-S6	115.9(2)	C3-C4-S6	114.2(2)		
C3-C5-S4	127.1(2)	C3-C5-S2	115.5(2)		
S4-C5-S2	117.3(1)	C4-C6-S8	135.0(2)		
C4-C6-S7	114.0(2)	S8-C6-S7	110.5(2)		

that it is square planar both in the solid state and in solution. The ^{13}C NMR spectrum of $\text{Pt}(\text{C}_6\text{S}_8)_2^{2-}$ shows signals for both the organic cation and the inorganic anion, the latter consisting of three signals.

Discussion

The bicyclic species C_6S_8 is an unusual example of an electroactive inorganic heterocycle whose redox properties are noteworthy in the context of S-S containing species. While the structure of C_6S_8 was not determined directly, its analogue $\text{C}_6\text{S}_6\text{O}_2$ was fully characterized. A close structural similarity of the bis(*trithiocarbonate*) C_6S_8 and the bis(*dithiocarbonate*) $\text{C}_6\text{S}_6\text{O}_2$ is supported by the fact that the dioxo species is generated in good yield from **1**. Furthermore, the structure of the dianion $\text{C}_6\text{S}_8^{2-}$ is that expected to result by cleavage of the S-S bond in **1**. Finally the close structural relationship between **1** and **2** is indicated by the similar electrochemical properties of $\text{C}_6\text{S}_6\text{O}_2^{2-}$ and $\text{C}_6\text{S}_8^{2-}$. Crystallographic and ^{13}C NMR analyses clearly show that the reduction of **1** and **2** is accompanied by scission of the S-S bond. The reduction of the S-S bond in 1,2-dithiins had not been previously observed.^{22,23}

Compounds **1** and **2** are most distinctive because their S-S bonds can be reversibly reduced, not only chemically but also on the relative short time scale of cyclic voltammetry. The reversibility of the reduction process is attributable to the intramolecular nature of the S-S forming process. Other examples of the reversible intramolecular scission of disulfides are known, e.g., $\text{Fe}_2\text{S}_2(\text{CO})_6^{24}$ and its inorganic analogue FeS_2 ,²⁵ but these require potent reductants, e.g., Na. Furthermore the oxidative coupling of thiolates on the time scale of cyclic voltammetry is quite uncommon.

(19) Studies of Brietzer, J. G.; Chou, J.-H.; Smirnov, A.; Szczepura, L. F.; Rauchfuss, T. B.

(20) Qualitative measurements suggest that $[\text{Ni}(\text{C}_6\text{S}_6\text{O}_2)_2]^{2-}$ forms analogously.

(21) Coucouvanis, D.; Murphy, C. N.; Simhon, E.; Stremple, P.; Draganjac, M. *Inorg. Synth.* **1982**, *21*, 23 and references therein.

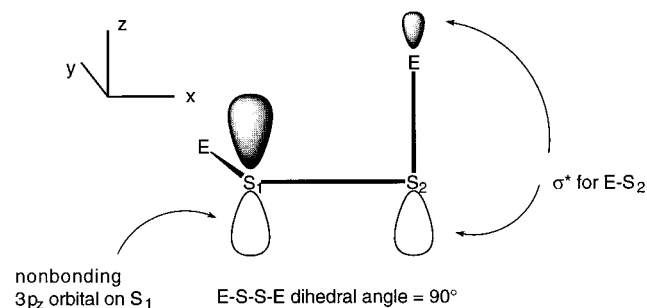
(22) Freeman, F.; Kim, D. S. H. L.; Rodriguez, E. *Sulfur Reports* **1989**, *9*, 207.

(23) Recent work on the chemistry of 1,2-dithiins: Block, E.; Page, J.; Toscano, J. P.; Wang, C.-X.; Zhang, X.; DeOrazio, R.; Guo, C.; Sheridan, R. S.; Towers, G. H. N. *J. Am. Chem. Soc.* **1996**, *118*, 4719.

(24) Weatherill, T. D.; Rauchfuss, T. B.; Scott, R. A. *Inorg. Chem.* **1986**, *25*, 1466.

(25) Peled, E.; Golodnisky, D.; Ardel, G.; Lang, J.; Lavi, Y. *J. Power Sources* **1995**, *54*, 496.

Another noteworthy aspect of the redox chemistry of **1** and **2** is the mildness of the redox potentials, which are within 100 mV of SCE. Most organic disulfides require ~ 0.5 V more driving force to effect reduction. One factor favoring reduction is the electron withdrawing character of the 1,3-dithiacyclopentene-2-thione substituents.²⁶ The redox potential might also be influenced by the strain associated with the small dihedral angle for the central C-S-S-C linkage in **2** (and **1**). This angle is normally near 90° for acyclic disulfides.²⁷ The preference for 90° dihedral angles has been much discussed.²⁸ More recent discussions have pointed out that 90° dihedral angles maximize overlap of the C-S σ^* orbital and an otherwise nonbonding 2p electrons ("lone pair") on sulfur.^{29,30} This



explanation is consistent with the finding that stabilization increases with the electronegativity of R,³¹ since the energy of the σ^* level will be lower for electronegative R. The stabilization arising from 90° dihedral angles is supported by studies on the rotational barriers for S-S bonds in R_2S_2 .³¹ For organic disulfides, these barriers approach 6 kcal/mol.³²

To appreciate the high oxidizing power of **1** and **2**, it is instructive to review the redox properties of other disulfides (Table 4). At pH = 7, organic disulfides typically reduce within 100 mV of -0.25 V, e.g., -0.19 V for Ph_2S_2 and -0.32 V for lipoic acid (vs NHE). In contrast, the inorganic disulfides discussed in this work are reduced at 0.331 (C_6S_8) and 0.171 V ($\text{C}_6\text{S}_6\text{O}_2$). Thus, these new species are more than 0.5 V more oxidizing than organic disulfides. Again reflecting their electronegative character of these species, the dithiolates are not readily protonated. Thus the redox for **1** and **2** is uncomplicated by protonation, in contrast to the situation for conventional organic disulfides. Polarographic studies show that the oxidation $(\text{NC})_2\text{C}_2\text{S}_2^{2-/-}$ (where $(\text{NC})_2\text{C}_2\text{S}_2^{2-}$ is the maleonitriledithiolate or mnt^{2-}) occurs at 0.321 V to give the acyclic disulfide $[(\text{CN})_2\text{C}_2\text{S}_2]_2^{2-}$, thus the resulting disulfide is more oxidizing than **1** by ca. 150 mV.³³ In contrast to **1**, however, the oxidized form of this cyano-substituted 1,2-dithiolate, i.e., $[\text{mnt}^0]_n$, is too unstable for isolation.

The small separation of the two redox processes, $\Delta E_{1/2}$, for **1** and **2** is also unusual, but there are few precedents in sulfur

(26) The acceptor properties of the $\text{C}_3\text{S}_5^{2-}$ ligand have been evaluated through electrochemical studies on a series of $\text{Mo}(\text{dithiolene})_3$ complexes: Yang, X.; Freeman, G. K. W.; Rauchfuss, T. B.; Wilson, S. R. *Inorg. Chem.* **1991**, *30*, 3034.

(27) Singh, R.; Whitesides, G. M. *J. Am. Chem. Soc.* **1990**, *112*, 6304.

(28) Steudel, R. *Angew. Chem., Int. Ed. Engl.* **1975**, *14*, 655.

(29) Steudel, R.; Drozdova, Y.; Miaskiewicz, K.; Hertwig, R. H.; Koch, W. *J. Am. Chem. Soc.* **1997**, *119*, 1990 and references therein.

(30) More detailed analyses of polysulfanes suggest that the most stable dihedral angles deviate from 90° by 10° . See: Drozdova, Y.; Miaskiewicz, K.; Steudel, R. *Z. Naturforsch.* **1995**, *50b*, 889.

(31) For example see the results of DNMR studies on EtOSSOEt : Seel, F.; Gombler, W.; Budenz, R. *Liebigs Ann. Chem.* **1970**, *735*, 1. Seel, F.; Budenz, R.; Gombler, W. *Z. Naturforsch.* **1970**, *25b*, 885.

(32) Fraser, R. R.; Boussard, G.; Saunders, J. K.; Lambert, J. B.; Mixan, C. *J. Am. Chem. Soc.* **1971**, *93*, 3822.

(33) McCleverty, J. A. *Prog. Inorg. Chem.* **1968**, *10*, 49.

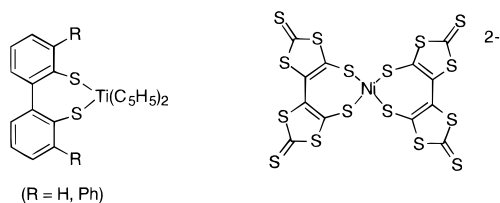
Table 4. Redox Potentials for Selected Disulfides

disulfide	$E_{1/2}$ (V vs NHE)	method and conditions	ref
(C ₂ N ₂ S)(SLi) ₂ /[(C ₂ N ₂ S) ₂] (dimercaptodithiazole) _n	~ -0.04 ^a	vs Li ^{0/+} (open circuit voltage)	DeJonge ⁸
C ₂ H ₄ (SH) ₂ /(SC ₂ H ₄ S) _n (ethanedithiol) _n	-0.239	K_{eq} vs lipoic acid	Lees and Whitesides ^d
(NC) ₂ C ₂ S ₂ ^{-/2-} (maleonitrile dithiolate) (pH 5)	0.321 ^b	polarography	McCleverty ³³
dihydrolipoic/acid/lipoic acid (pH 7)	-0.294	(pH 7.1, 22 °C)	Sanadi et al. ^h
C ₇ H ₁₅ SH/(C ₇ H ₁₅ S) ₂ (pH 7)	-0.261	K_{eq} vs lipoic acid	Lees and Whitesides ⁸
PhSH/Ph ₂ S ₂ (pH 7)	-0.245	K_{eq} vs lipoic acid	Lees and Whitesides ⁸
C ₆ S ₈ ^{0/-/2-}	0.331, 0.181 ^c	this work	this work
C ₆ S ₆ O ₂ ^{0/-/2-}	0.171, 0.031 ^d	this work	this work
S ₈ /2S ₃ ⁻	-0.36 ^e	CV ^f	Sawyer et al. ^f

^a Open circuit voltage (OCV) quoted was corrected to NHE by subtracting 3.04 V (for Li^{0/+}) from the published values. ^b 0.08 V vs SCE ((NC)₂C₂S₂)₂⁰ is unstable and has not been characterized electrochemically). ^c 0.09, -0.06 V vs SSCE. ^d -0.07, -0.21 V vs SSCE. ^e 0.6 V vs sce. ^f DMSO soln at Au. ⁸ Lees, W. J.; Whitesides, G. M. *J. Org. Chem.* **1993**, *58*, 642. ^h Sanadi, D. R.; Langley, M.; Searls, R. L. *J. Biol. Chem.* **1959**, *234*, 178. ^h Martin, R. P.; Doub, W. H., Jr.; Roberts, J. L., Jr.; Sawyer, D. T. *Inorg. Chem.* **1973**, *12*, 1921. Fujinaga, T.; Kuwamoto, T.; Okazaki, S.; Hojo, M. *Bull. Soc. Chem. Jpn.* **1980**, *53*, 2851. Hojo, M.; Sawyer, D. T. *Inorg. Chem.* **1989**, *28*, 1201. Gaillard, F.; Levillain, E. *J. Electroanal. Chem.* **1995**, *398*, 77.

chemistry, partly because of the interfering effects of protonation, which in turn is due to the high basicity of most thiolates. Small values of $\Delta E_{1/2}$ typically indicate either a (fast) chemical rearrangement that encourages the second redox process or low on-site Coulomb energy, which essentially means that the charges are effectively dispersed such that the effect of the first reduction (or oxidation) does not inhibit the second step.³⁴ The latter explanation would be consistent with the π -delocalized character of the carbon sulfide framework. An additional factor that facilitates the second reduction is the possibility of strain inherent in **1** and **2** by virtue of the small C-S-S-C dihedral angle.

The lack of reversible redox activity in the complexes [M(C₆S₈)₂]²⁻ reaffirms the central importance of the S-S bond in the behavior of **1** and **2**. These ligands are potentially interesting as homologs of the dithiolene (1,2-alkenedithiolate) ligands. The 1,2-dithiolenes are renown as "noninnocent" due to their ability to stabilize metals in multiple oxidation states by virtue of the strong M-S π interactions.³⁵ In contrast, the 1,4-dithiolenes reported in this work appear to serve as innocent, chelating thiolates, perhaps due to the incompatibility of the nonplanar MS₂C₄ ring³⁶ with π -delocalization. We have previously reported a second family of 1,4-dithiolene complexes in the form of their titanocene derivatives which, like **3** and **4**, feature seven-membered MS₂C₄ rings:



Because C₆S₈²⁻ is easily prepared, this class of ligands may be of further interest as precursors to metal dithiolates with large S-M-S angles.

Experimental Section

Materials and Methods. All reagents and inorganic salts were used as received, while solvents were dried and deoxygenated by standard methods. We synthesized C₃S₅²⁻ by the addition of DMF to a suspension of Na in CS₂.³⁷

(34) Stafford, P. R.; Rauchfuss, T. B.; Verma, A. K.; Wilson, S. R. *J. Organomet. Chem.* **1996**, *526*, 203.

IR spectra were recorded on KBr disks and are reported in cm⁻¹. IR and ¹³C NMR absorptions for PPh₄⁺ cation are seen in all samples at 527, 688, 722, 750, 942, 1107, and 1439 cm⁻¹ and at δ 117.6 (d), 130.5 (d), 134.5 (d), and 135.4 (d), respectively.

Electrochemical measurements were conducted in a three-electrode one compartment cell containing a glassy carbon working electrode, a saturated sodium calomel electrode (0.2360 V vs NHE) reference electrode, and a Pt auxiliary electrode in 0.2 M Bu₄NPF₆ in DMF. Cyclic voltammetric measurements were measured at a scan rate of 100 mV/s, and differential pulse voltammograms were measured at a scan rate of 20 mV/s with a pulse amplitude of 10 mV, a pulse width of 50 ms, and a pulse period of 100 ms.

(PPh₄)₂[C₆S₈]. A dark purple suspension of 0.328 g (1 mmol) of C₆S₈ in 30 mL of THF was cooled with an acetone-dry ice bath and treated dropwise with 2.2 mL of 1 M THF solution of LiBHET₃. The color of the solution changed to violet red almost immediately. The THF was removed under vacuum and 50 mL of O₂-free water was added to redissolve the dark brown residue. A solution of 0.75 g (2 mmol) of PPh₄Cl in 30 mL of O₂-free water was added to the dark brown solution to give a violet microcrystals. The crude solid was washed with water and dried under vacuum. Yield: 0.985 g (98%). X-ray quality crystals were grown by fractional crystallization from DMF/Et₂O as violet platelike crystals. Alternatively, the reduction of the C₆S₈ can be achieved by using Na metal in liquid NH₃. IR: 1365, and 1024 (ν_{C-S}). ¹³C NMR (DMF): δ 207.3 (s), 159.2 (s), and 123.7 (s) assigned to the C₆S₈²⁻ dianion. Anal. Calcd for C₅₄H₄₀P₂S₈: C, 64.4; H, 3.97; S, 25.47. Found: C, 64.70; H, 3.99; S, 25.11.

(PPh₄)₂[C₆S₆O₂]. A suspension of 0.317 g (1.1 mmol) of C₆S₆O₂ in 30 mL of THF was treated with 3.5 mL of a 1.0 M THF solution of LiBHET₃ at -78 °C. The orange solid slowly dissolved to give a yellow brown solution. The solvent was removed under reduced pressure as the solution was warmed to room temperature. The remaining oil was extracted with 25 mL of O₂-free H₂O. A solution of 1.3 g of PPh₄Cl in 25 mL of H₂O was added to precipitate the desired product, (PPh₄)₂[C₆S₆]. This material was purified by reprecipitation from DMF solution by the addition of Et₂O. Yield: 760 mg (75%). IR: 1417, 1595 (ν_{CO}). ¹³C NMR (DMSO-*d*₆): δ 196.6 (s), 148.4 (s), and 111.6 (s). Anal. Calcd for C₅₄H₄₀O₂P₂S₆: C, 66.50; H, 4.13; S, 19.7. Found: C, 66.52; H, 4.00; S, 19.24.

(PPh₄)₂[Ni(C₆S₈)₂]. A solution of 210 mg (0.2 mmol) of (PPh₄)₂[C₆S₈] in 30 mL of DMF was treated dropwise with a solution of 24 mg (0.1 mmol) of [Ni(H₂O)₆]Cl₂ in 20 mL of MeOH. The color of the solution changed from violet to dark brown upon the addition, and dark brown microcrystals start to precipitate out of the solution. The

(35) For leading references, see Houser, E. J.; Venturelli, A.; Rauchfuss, T. B.; Wilson, S. R. *Inorg. Chem.* **1995**, *34*, 6402.

(36) Mueller-Westerhoff, U. T.; Vance, B. In *Comprehensive Coordination Chemistry*; Wilkinson, G.; Gillard, R. D.; McCleverty, J. A., Eds.; Pergamon: Oxford, 1987.

Table 5. Crystal and Data Collection Details for C₆S₆O₂, (PPh₄)₂C₆S₈, and (PPh₄)₂[Ni(C₆S₈)₂]

formula	C ₆ S ₆ O ₂	C ₅₄ H ₄₀ P ₂ S ₈	C ₆₀ H ₄₀ NiP ₂ S ₁₆
fw	296.42	1007.28	1394.54
<i>a</i> , Å	3.9187(2)	10.5473(3)	10.4752(1)
<i>b</i> , Å	14.9734(6)	11.1366(3)	12.6907(1)
<i>c</i> , Å	16.1293(7)	11.2658(3)	23.5042(3)
α, deg	90.00	95.165(1)	90.00
β, deg	90.00	112.218(1)	101.760(1)
γ, deg	90.00	102.225(1)	90.00
<i>Z</i> , V, Å ³	4, 946.41(7)	2, 1175.91(6)	4, 3059.01(5)
space group	<i>P</i> 2 ₁ 2 ₁ 2 ₁ (no. 19)	<i>P</i> $\bar{1}$ (no. 2)	<i>P</i> 2 ₁ / <i>n</i> (no. 14)
color, habit	orange, needle	purple, plate	brown, plate
<i>D</i> _{cal} , g/cm ³	2.080	1.422	1.514
radiation	Mo Kα	Mo Kα	Mo Kα
μ, mm ⁻¹	1.406	0.487	0.956
2θ _{max} , deg	56.56	56.56	56.56
absorption correction	integration	integration	integration
index ranges	-3 ≤ <i>h</i> ≤ 5 -18 ≤ <i>k</i> ≤ 19 -21 ≤ <i>l</i> ≤ 14	-13 ≤ <i>h</i> ≤ 5 -13 ≤ <i>k</i> ≤ 14 -14 ≤ <i>l</i> ≤ 15	-13 ≤ <i>h</i> ≤ 11 -16 ≤ <i>k</i> ≤ 14 -29 ≤ <i>l</i> ≤ 31
no. of data coll.	6226	7612	18837
unique reflections	2277	5281	7170
no. of variables	127	289	358
<i>R</i> ₁ / <i>wR</i> ₂ ^{a,b}	0.0468/0.0963	0.0326/0.0878	0.0367/0.0840
(<i>F</i> > 4σ(<i>F</i>))			

$$^a R_1 = \sum(|F_o| - |F_c|)/\sum|F_o| \text{ for } F > 4\sigma(F). \quad ^b wR_2 = [\sum[w(F_o^2 - F_c^2)^2]/\sum[w(F_o^2)^2]]^{1/2}.$$

solution was left to stir for an additional 30 min, and the solid was collected through filtration and washed thoroughly with MeOH and ether. Yield: 105 mg (75%). X-ray quality crystals were grown by fractional crystallization from DMF/Et₂O as dark reddish brown platelike crystals. IR: 1060 (*ν*_{C=S}). Anal. Calcd for C₆₀H₄₀NiP₂S₁₆: C, 51.67; H, 2.89; Ni, 4.21; S, 36.78. Found: C, 51.52; H, 2.77; Ni, 4.06; S, 36.59.

(PPh₄)₂[Pt(C₆S₈)₂]. A solution of 100 mg (0.24 mmol) of K₂[PtCl₄] in 50 mL of H₂O was added to a solution of 400 mg (0.49 mmol) of (PPh₄)₂[C₆S₈] in 115 mL MeOH, and the mixture was refluxed for 1 h. The rust-colored solid was filtered off, washed with H₂O, and air-dried. This solid was extracted into 50 mL of CH₂Cl₂ and reprecipitated by the addition of 30 mL of EtOH and subsequent reduction in volume. The sample was recrystallized from DMF–Et₂O. Yield: 70 mg (30%). IR: 1056 (*ν*_{C=S}). ¹³C NMR (DMSO-*d*₆): δ 209.7 (s), 144.6 (s) and 124.8 (s) assigned to [Pt(C₆S₈)₂]²⁻. Anal. Calcd for C₆₀H₄₀P₂PtS₁₆: C 47.07; H, 2.63; Pt, 12.74; S 33.50. Found: C, 47.14; H, 2.56; Pt, 12.51; S, 33.33.

Crystallographic Analysis of C₆S₆O₂. Orange needlelike crystals of C₆S₆O₂ were grown by fractional diffusion of Et₂O into CH₂Cl₂ solution of C₆S₆O₂. The data crystal was attached to a thin glass fiber using Paratone-N oil (Exxon). The data crystal was bound by the (1 0 0), (-1 0 0), (0 1 0), (0 -1 0), (0 0 1), and (0 0 -1) faces. Distances from the crystal center to these facial boundaries were 0.020, 0.020, 0.040, 0.040, 0.240, and 0.240 mm, respectively. Diffraction data were collected at 198 K on a Siemens 3-circle platform diffractometer with CCD area detector. Crystal and refinement details are given in Table 5. Systematic conditions suggested the orthorhombic space group *P*2₁2₁2₁ (no. 19). Three standard intensities monitored every 90 min showed no decay. Step-scanned intensity data were reduced by profile analysis³⁸ and corrected for Lorentz-polarization effects and for absorption (SHELXTL version 5.03). Scattering factors and anomalous dispersion terms were taken from standard tables.³⁹

The structure was solved by Direct Methods⁴⁰ and refined by full-matrix least squares on *F*² (SHELXL 93).⁴¹ All atoms were refined with anisotropic thermal coefficients. The highest peak in the final map had no significant unassigned features. A final analysis of variance between observed and calculated structure factors showed no dependence on amplitude or resolution.

(37) Yu. L.; Zhu, D. *Phosphorus, Sulfur, Silicon* **1996**, 116, 225.

(38) Coppens, P.; Blessing, R. H.; Becker, P. *J. Appl. Crystallogr.* **1972**, 7, 488.

(39) (a) *International Tables for X-ray Crystallography*; Wilson, A. J. C., Ed.; Kluwer Academic Publishers: Dordrecht, Netherlands, 1992; Vol. C. scattering factors, pp 500–502. (b) *International Tables for X-ray Crystallography*; Wilson, A. J. C., Ed.; Kluwer Academic Publishers:

Crystallographic Analysis of (Ph₄P)₂[C₆S₈]. Purple-red platelike crystals of were grown by fractional diffusion of Et₂O into a DMF solution of (Ph₄P)₂[C₆S₈]. The data crystal was attached to a thin glass fiber using Paratone-N oil (Exxon). The data crystal was bound by the (1 0 0), (-1 0 0), (0 0 1), (0 0 -1), (0 1 0), (0 -1 0), (0 -1 1), and (-1 1 0) faces. Distances from the crystal center to these facial boundaries were 0.130, 0.130, 0.120, 0.120, 0.250, 0.250, 0.200, and 0.200 mm, respectively. Diffraction data were collected at 198 K on a Siemens 3-circle platform diffractometer with CCD area detector. Crystal and refinement details are given in Table 5. Systematic conditions suggested the ambiguous space group *P* $\bar{1}$ (no. 2). Three standard intensities monitored every 90 min showed no decay. Step-scanned intensity data were reduced by profile analysis³⁸ and corrected or Lorentz and polarization effects and for absorption (SHELXTL version 5.03). Scattering factors and anomalous dispersion terms were taken from standard tables.³⁹

The structure was solved by direct methods⁴⁰ and refined by full-matrix least squares on *F*² (SHELXL 93).⁴¹ Correct positions for all nonhydrogen atoms were deduced from a vector map. H atoms *U*'s were assigned as 1.2 times *U*_{eq} of the adjacent non-H atoms. All non-hydrogen atoms were refined with anisotropic thermal coefficients. The highest peak in the final map had no other significant features. A final analysis of variance between observed and calculated structure factors showed no dependence on amplitude or resolution.

Crystallographic Analysis of (Ph₄P)₂[Ni(C₆S₈)₂]. Dark-brown crystals were grown by fractional diffusion of Et₂O into a DMF solution of (Ph₄P)₂[Ni(C₆S₈)₂]. The data crystal was attached to a thin glass fiber using Paratone-N oil (Exxon). The data crystal was bound by the (0 0 1), (0 0 -1), (0 1 1), (0 -1 -1), (-2 -1 0) and (1 -1 0) faces. Distances from the crystal center to these facial boundaries were 0.18, 0.18, 0.28, 0.28, 0.32, and 0.24 mm, respectively. Diffraction data were collected at 198 K on a Siemens 3-circle platform diffractometer with CCD area detector. Crystal and refinement details are give in Table 5. Systematic conditions suggested the space group *P*2₁/*n* (no. 14). Three standard intensities monitored every 90 min showed no decay of the crystal. Step-scanned intensity data were reduced by profile analysis³⁸ and corrected for Lorentz-polarization effects and for absorption. Scattering factors and anomalous dispersion terms were taken from standard tables.³⁹

The structure was solved by direct methods⁴⁰ and refined by full-matrix least squares on *F*² (SHELXL 93).⁴¹ Correct positions for all

Dordrecht, Netherlands, 1992; Vol. C. dispersion corrections, pp 219–222.

(40) Sheldrick, G. M. SHELXS–86. *Acta Crystallogr.* **1990**, A46, 467. Egert, E.; Sheldrick, G. M. *Acta Crystallogr.* **1985**, A41, 262.

(41) Sheldrick, G. M. SHELXS–93.

nonhydrogen atoms were deduced from a vector map. H atoms U^s were assigned as 1.2 times U_{eq} of the adjacent non-H atoms. All nonhydrogen atoms were refined with anisotropic thermal coefficients. The highest peak in the final map had no other significant features. A final analysis of variance between observed and calculated structure factors showed no dependence on amplitude or resolution.

Acknowledgment. This work was supported by the U.S. Department of Energy, Division of Materials Science Grant DEFG02-96ER45439 through the University of Illinois at Urbana-Champaign, Frederick Seitz Materials Research Labora-

tory. The National Science Foundation (CHE-9504647) also provided partial support including a postdoctoral fellowship for L.F.S. We thank Theresa Prussak for collection of the crystallographic data.

Supporting Information Available: Crystallographic data for compounds **2**, $(PPh_4)_2[1]$, and **3** including positional and thermal parameters (13 pages). See any current masthead page for ordering and Internet access instructions.

JA973186J